Food Sci. Technol. Res., **12** (2), 96–100, 2006

Foreign Substance Detection in Blueberry Fruits by Spectral Imaging

Mizuki TSUTA[1]*, Tomohiro TAKAO[2], Junichi SUGIYAMA[1], Yukihiro WADA[2] and Yasuyuki SAGARA[3]

[1] *Food Engineering Division, National Food Research Institute, 2-1-12 Kan-nondai, Tsukuba, Ibaraki 305-8642, Japan*
[2] *NISSEI Co., Ltd., 445-1 Miyazawa, South Alps, Yamanashi 400-0415, Japan*
[3] *Graduate School of Agricultural and Life Sciences, The University of Tokyo, 1-1-1 Yayoi, Bunkyo, Tokyo 113-8657, Japan*

Received August 5, 2005; Accepted April 6, 2006

Spectral analysis and image processing of the spectral images of blueberries and several foreign substances clarified that plant organs could be detected by the second derivative absorbance image at 680 nm, which is an absorption band of chlorophyll. As a feasibility study, spectral images of blueberries and plant organs placed in the 160×120 mm area were acquired at 660, 680 and 700 nm in order to develop a second derivative absorbance image at 680 nm. Then the second derivative absorbances of 52 blueberries and 26 plant organs in the image and their mean values were calculated. Using these data, the probability of being a plant organ, *p*, was calculated for each pixel of the second derivative absorbance image in order to develop a plant organ detection image. In the detection image, a pixel with *p* value larger than 0.95 was judged as a plant organ. The positions of pixels judged as plant organs in the detection image were in good agreement with the actual locations where plant organs had been placed. Therefore, it could be concluded that plant organs contaminated raw blueberry materials could be detected using the method developed in this research.

Keywords: foreign substance, detection, spectral imaging, blueberry

Introduction

In Japan, complaints from consumers about foreign substances contaminating fruit processed products, such as jam and fruit sauce, have been increasing because of the rise in concerns of consumers about food safety and quality. Therefore, visual inspections of raw fruit materials have been performed in fruit processing factories. However, it is hard to detect foreign substances completely by human eyes because they are dyed in the same color as the raw fruit material by its juice and are thus not distinguishable by color.

In contrast, spectral imaging has been attracting attention as a novel visualization technique. This technique involves taking the images of an object at various wavelengths at a few nm intervals and acquiring spectral and spatial information simultaneously. Because of the inherent advantage of a high wavelength resolution over the image acquisition process of human eyes which is based on RGB-cones, something invisible to the naked eye, such as the distribution of a constituent in food or the internal structure of food, can be visualized using this technique (Do *et al.*, 2005; Martinsen and Schaare, 1998; Miyashita *et al.*, 2004; Sugiyama, 1999; Tsuta *et al.*, 2002a; Tsuta *et al.* 2002b; Tsuta *et al.*, 2004). Therefore, it was considered that foreign substances undetectable by visual inspections could be detected by applying this technique.

In this study, blueberries were selected as a sample because their functionality has attracted Japanese consumers and their imports have been increasing. The aim of this study was to develop a basic foreign substance detection method for raw blueberries using a spectral imaging technique. A feasibility study was also carried out in order to improve the detection method and to confirm the possibility of its application to the actual blueberry processing factories.

* To whom correspondence should be addressed.
E-mail: mizukit@affrc.go.jp

Materials and Methods

Sample Frozen blueberries imported from USA were left at room temperature for two hours to be defrosted. Plant organs of blueberry such as leaves and twigs, stones and worms found in a blueberry-processing factory, and human hairs acquired from researchers at National Food Research Institute were prepared as foreign substances. The foreign substances were dyed in the same color as blueberries by soaking them in the blueberry juice, which had exuded from the blueberries during the defrosting process, for 30 minutes.

Spectral Imaging System A spectral imaging system shown in Fig. 1 was utilized in order to acquire spectral images of the sample. The system was composed of an illuminator (Megalight 50, Hoya-Schott Corp., Japan), a stereoscopic microscope (MZ-FLIII, Leica Microsystems, Japan), a liquid crystal tunable filter (LCTF; VS-VIS2-10-MC-35, Cambridge Research & Instrumentation Inc., USA) and a monochrome CCD camera (ORCA-ER-1394, Hamamatsu Photonics K.K., Japan). A 1.25x objective lens was attached to the microscope so that a 12×9 mm area could be observed. By changing the voltage applied to LCTF, the wavelength of light transmitted through LCTF could

be selected from 400 to 720 nm, with the bandwidth of 10 nm and the wavelength accuracy of 1.25 nm. The CCD camera had 1,344×1,024 pixels (1.3 mega pixels) and its gradation was 12 bit (4,096 steps). Using this spectral imaging system, the spectral images at specific wavelengths of a sample under the objective lens could be acquired.

Preliminary Experiment A preliminary experiment was carried out in order to develop a basic foreign substance detection method and to select the most suitable foreign substance for the feasibility study. Defrosted blueberries were placed in a disposable balance dish (D-M, INA-OPTIKA Co., Ltd., Japan) and dyed foreign substances were placed on top of the blueberries as shown in Fig. 1. Samples 1 and 2, which were prepared in this way, were utilized as model samples in order to represent the difficulty in detecting these foreign substances in blueberry processing factories. On the other hand, because it was hard to acquire absolute absorbance of samples, a ceramic board was prepared as a white standard for relative absorbance calculations. The ceramic board was set under the imaging system and the position of the illuminator was adjusted so that its surface illuminated uniformly. The spectral images of the ceramic board were acquired in the wavelength range from 405 to 720 nm at five nm intervals. Then, as shown in Fig. 2, the ceramic board was replaced with the sample and spectral images of the sample were acquired at the same condition as the white reference.

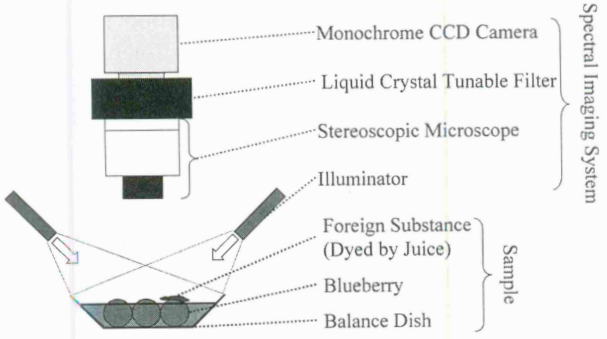

Fig. 1. Outline of Preliminary Experiment.

Spectral Analysis Spectral images of the sample and the white reference include: (1) thermal noise, (2) bias signals to offset the CCD slightly above zero A/D counts, (3) sensitivity variations from pixel to pixel on the CCD, and (4) lighting variations on the samples surface (Fukushima, 1996). To compensate for these effects, noise and shading corrections described in a previous paper (Sugiyama, 1999) were performed for all images. Next, the average intensity of pixels of a blueberry in the compensated image at 405 nm (*Is (405)*) was calculated as shown in Fig. 3. The average intensity of the pixels in the same area of the white standard image at 405 nm (*Iw (405)*) was also calculated. Then, the relative absorbance of the blueberry at 405 nm (*A (405)*) was calculated from the equation shown below.

$$A(405) = log(Iw(405)/Is(405)) \qquad \text{Eq. (1)}$$

These calculations were applied to the spectral images at the wavelengths from 410 to 720 nm in order to acquire the absorbance spectra of the blueberry. Absorbance spectra of other blueberries and foreign substances were calculated similarly. These spectra were differentiated twice because the second derivative method has following merits (Iwamoto *et al*, 1994; Morimoto *et al.*, 2001): (1) positive peaks in a raw spectrum are converted into negative peaks in a second derivative spectrum, (2) the resolution is en-

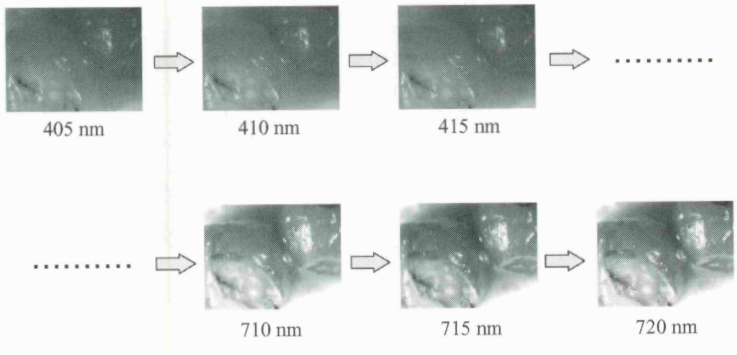

Fig. 2. Acquisition of Spectral Images.

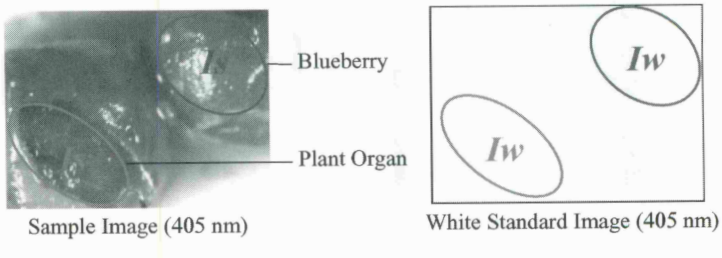

Fig. 3. Absorbance Calculation.

hanced for the separation of overlapping peaks and the emphasis of small peaks, (3) the additive and multiplicative baseline shifts in a raw spectrum are removed. The differentiation of the spectra was carried out by applying the equation shown below.

$$d^2A_i=(A_{i+k}-A_i)+(A_i-A_{i-k})=A_{i+k}-2\times A_i+A_{i-k} \quad \text{Eq. (2)}$$

Where A_i is the absorbance at i nm, d^2A_i is the second derivative absorbance at i nm, and k is the distance between the neighboring wavelengths, which is called a derivative gap. In this study, k was set to 20 nm considering the following two factors: (1) it was twice as large as the bandwidth of LCTF and thus no overlap between the acquired absorbances at neighboring wavelengths was expected. (2) a small gap was needed because the larger the gap, the bigger the difference in the sensitivity of the spectral imaging system between the neighboring wavelengths. Equation (2) indicates that absorbances at three wavelengths of i, $i+k$ and i-k are sufficient for calculating the second derivative absorbance at i nm. By examining the absorbance and second derivative absorbance spectra, the wavelengths at which the difference in absorbance between the blueberries and foreign substances was sufficiently clear to distinguish between them, were specified.

Image Processing As shown in Fig. 4, the absorbance of each pixel in the spectral images at the specified wavelengths were calculated similarly using Eq. (1) in order to develop absorbance images in which absorbance of each pixel was indicated as its intensity. The second derivative absorbances of each pixel at the specified wavelengths were calculated by applying Eq. (2) to neighboring three absorbance images. Using image-processing software (Adobe Photoshop 7.0, Adobe Systems Inc., USA), the absorbance and second derivative absorbance images were converted into bitmap images. These images were then binarized in order to create foreign substance detection images in which the pixels of the foreign substances and all other pixels were exhibited as white and black spots, respectively. The white pixels in the detection images were compared with the positions where the foreign substances were actually placed in order to determine the detection accuracy. Finally, the most appropriate foreign substance for the feasibility study was selected based on the detection accuracy and the number of the complaints from consumers.

Feasibility Study The stereoscopic microscope of the imaging system was replaced with a camera lens (FD28 mm F3.5 S.C., Canon, Tokyo, Japan) and 160×120 mm area could be observed using this system. As a model sample of blueberries on the belt conveyer in a blueberry-processing factory, defrosted blueberries were placed on a 300 ×300 mm white standard board. Then dyed plant organs, which were selected as the foreign substances for the feasibility study, were placed on top of the blueberries. Using the spectral imaging system, the spectral images of the sample at wavelengths at which plant organs could be detected (660, 680 and 700 nm), were acquired in a manner similar to the preliminary experiment.

Development of Foreign Substance Detection Criterion The absorbances of 52 blueberries and 26 plant organs at 660, 680 and 700 nm were calculated after noise and shading corrections of the acquired spectral images. The absorbances were then converted into the second derivative absorbances at 680 nm by applying Eq. (2). As a next step, a statistical criterion for the detection of plant organs was developed using a statistical analysis software (JMP 5.1, SAS Institute Inc., USA) because the basic foreign substance detection by the simple binarization method was considered to be not sufficiently reliable for practical use. First, the average value of the second derivative absorbances of blueberries ($d^2A_b(680)$) and plant organs ($d^2A_p(680)$) was calculated as shown in Fig. 5. Next, the square distance from each sample to $d^2A_b(680)$, $SqDist_b$ was calculated by squaring the difference between them. The square distance from each sample to $d^2A_p(680)$, $SqDist_p$ was also acquired. In addition, probability of being a plant organ, p was calculated by applying the equation shown below.

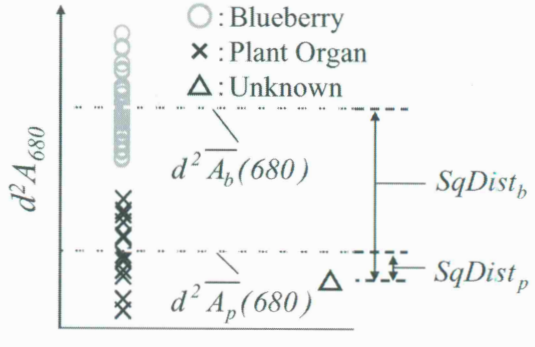

Fig. 5. Calculation of Square Distance.

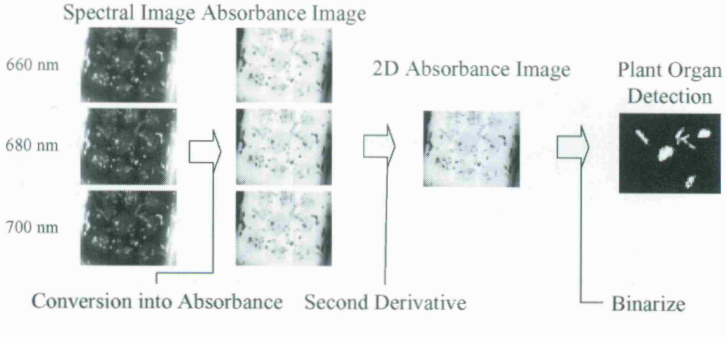

Fig. 4. Image Processing.

$$p = \frac{exp(-0.5 \times SqDist_p)}{exp(-0.5 \times SqDist_b) + exp(-0.5 \times SqDist_p)} \quad \text{Eq. (3)}$$

Finally, by applying a critical rate of 0.95, the criteria for the plant organs and other substances were set as follows.

$$p > 0.95 \Rightarrow Plant\ Organs \quad \text{Eq. (4)}$$

$$p \leq 0.95 \Rightarrow Others \quad \text{Eq. (5)}$$

Development of a Plant Organ Detection Image The second derivative absorbance image at 680 nm was developed using the image processing procedure of the preliminary experiment. Then, using an image processing software (Image Pro Plus 4.5, Media Cybernetics, USA) p of each pixel was calculated by applying Eq. (3) to each pixel. Finally, each pixel was assigned a specific color according to its p value as shown in Table 1 in order to develop a plant organs detection image.

Results and Discussion

Preliminary Experiment As a result of the absorbance calculation from the spectral images taken in the preliminary experiment, ten absorbance spectra from each category, that is, blueberry, plant organ, stone, hair and worm, were acquired. In order to examine the characteristic of each category, an average spectrum was calculated for each category as shown in Fig. 6. The absorbances of stones were larger than fruits at approximately 450 nm, and it was considered that stones could be detected by processing the absorbance image at this wavelength. On the other hand, as shown in Fig. 7, second derivative absorbance spectra were acquired by applying Eq. (2) to the absorbance spectra. The second derivative absorbance spectra of plant organs exhibited a strong negative peak at 680 nm, which was detected by processing the second derivative absorbance image at this wavelength.

Foreign Substance Selection for the Feasibility Study The absorbance image at 450 nm was converted into a bitmap image and binarized with a threshold value of 43 in order to develop a stone detection image as shown in Fig. 8. The threshold of the binarization was set to the middle of the intensities of stones and other substances in the bitmap image. The positions of white pixels in the image showed good coincidence with the actual locations

Table 1. Color Assignment According to p value.

p	Assigned Color
0.00 – 0.50	Blue
0.51 – 0.80	Sky Blue
0.81 – 0.90	Green
0.91 – 0.95	Yellow
0.96 – 1.00	Red

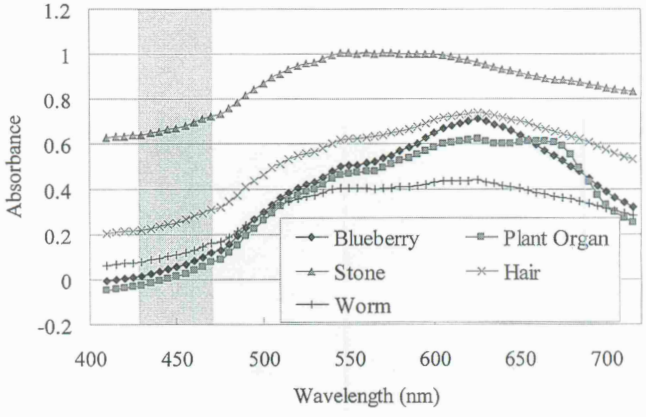

Fig. 6. Absorbance Spectra.

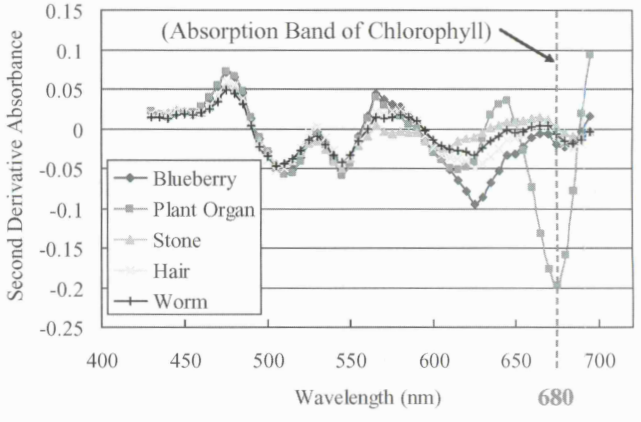

Fig. 7. Second Derivative Absorbance Spectra.

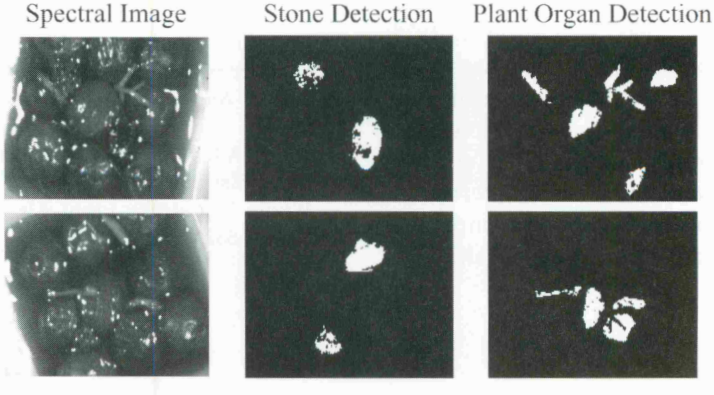

Fig. 8. Stone and Plant Organ Detection Images (Upper row: sample 1, Lower row: sample 2).

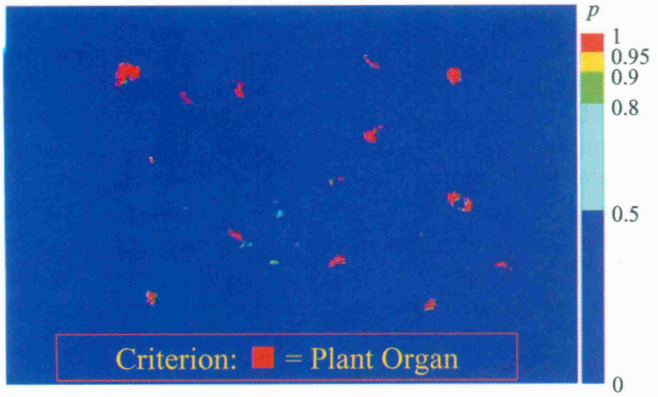

Fig. 9. Plant Organ Detection Image.

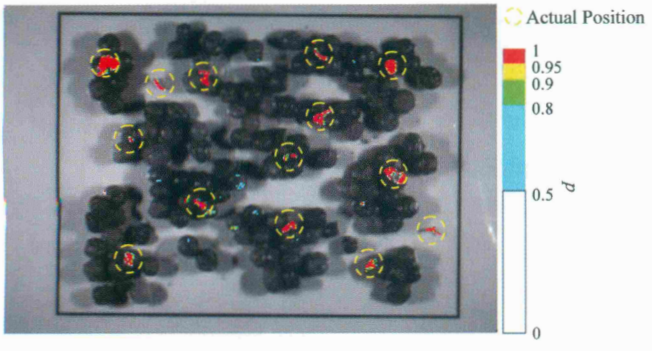

Fig. 10. Plant Organ Detection Image Superimposed on Spectral Images.

where stones had been placed. On the other hand, the second derivative absorbance image at 680 nm was binarized with a threshold value of 96 in order to acquire a plant organ detection image. Similar to the stone detection, the actual positions of plant organs were precisely reflected in the white pixels of the detection image. Therefore, it was concluded that stones and plant organs could be detected by applying the spectral imaging technique described above. However, neither a specific peak in the absorbance spectra of stones nor a clear factor, which could explain the difference in absorbance between stones and blueberries, was found. The strong negative peak at 680 nm, which was found in the second derivative absorbance spectra of plant organs, was considered to be derived from the absorption band of chlorophyll contained in them (Nussberger *et al*, 1994; Watada *et al.*, 1976). Moreover, the number of complaints from consumers about plant organs had been much greater than any other foreign substances. Therefore, plant organs were selected as a foreign substance sample for the feasibility study.

Plant Organ Detection Image The second derivative absorbance image at 680 nm of the feasibility sample was converted into a plant organ detection image as shown in Fig. 9. In this image, a red pixel could be considered as a plant organ according to the criterion of Eq. (4). The accuracy of the detection of plant organs was confirmed by superimposing the detection image on the accumulated raw spectral images as shown in Fig. 10. In this figure, pixels with p below 0.5 were made transparent so that blueberries and plant organs could be observed. Actual positions of plant organs were shown as yellow circles and the red part within each circle indicated the location of a plant organ. No red pixels were found outside the circles. Therefore, it was concluded that plant organs contaminated raw blueberry materials could be detected using the method developed in this research.

References

Do, G., Tsuta, M., Sugiyama, J., Ueno, S. and Sagara, Y. (2005). Three-Dimensional Visualization of Ice Crystals in Frozen Materials by Near-Infrared Imaging Spectroscopy. *Trans. of the JSRAE*, **22**, 185–191 (in Japanese).

Fukushima, H. (1996). Basics of Image Analysis. In "Reikyaku CCD nyuumon." Seibundou Sinkousha, Tokyo, Japan, pp. 133–181 (in Japanese).

Iwamoto, M., Kawano, S. and Uozumi, J. (1994). Data Processing Method. In "Kin-Sekigai Bunkouhou Nyuumon." Saiwai Shobou, Tokyo, Japan, pp 62–95.

Martinsen, P. and Schaare, P. (1998). Measuring Soluble Solid Distribution in Kiwifruit Using Near-Infrared Imaging Spectroscopy. *Postharvest Biology and Technology*, **14**, 271–281.

Miyashita, K., Tsuta, M., Suzuki, T., Do, G., Sugiyama, J., Nakauchi, S. and Shimizu, H. (2004). Visualization of the Internal Soybean Structure by the Three-Dimensional Spectral Imaging System (3D-SIS). *Nippon Shokuhin Kagaku Kogakkaishi*, **51**, 656–664 (in Japanese).

Morimoto, S., McClure, W.F. and Stanfield, D.L. (2001) Hand-Held NIR Spectrometry: Part I: An Instrument Based upon Gap-Second Derivative Theory. *Appl. Spectrosc.*, **55**, 182–189.

Nussberger, S., Dekker, JP., Kuhlbrandt, W., van Bolhuis, BM., van Grondelle, R. and van Amerongen, H. (1994). Spectroscopic Characterization of Three Different Monomeric Forms of the Main Chlorophyll a/b Binding Protein from Chloroplast Membranes. *Biochmistry*, **33**, 14775–14783.

Sugiyama, J. (1999). Visualization of Sugar Content in the Flesh of a Melon by Near-Infrared Imaging, *J. Agric. Food Chem.*, **47**, 2715–2718.

Tsuta, M., Sugiyama, J. and Sagara, Y. (2002). Near-Infrared Imaging Spectroscopy Based on Sugar Absorption Band for Melons. *J. Agric. Food Chem.*, **50**, 48–52.

Tsuta, M., Sugiyama, J. and Sagara, Y. (2002). Near-Infrared Imaging Spectroscopy Using a Hyper-Spectral Camera—Visualization of the Sugar Distribution in the Flesh of Melons—. *J. Inst. Image Inf. Telev. Eng.*, **56**, 2037–2040 (in Japanese).

Tsuta. M., Ichinose, S., Ogawa, F., Sugiyama, J. and Sagara, Y. (2004). Development and Application of a Multi-Band Image Scanner—Visualization of Sugar Distribution of Melons—. *Nippon Shokuhin Kagaku Kogakkaishi*, **51**, 247–253 (in Japanese).

Watada, A.E., Norris, K.H., Worthington, J.T. and Massie, D.R. (1976). Estimation of Chlorophyll and Carotenoid Contents of Whole Tomato by Light Absorbance Technique. *J. Food Sci.*, **41**, 329–332.